Design of a Novel In-Pipe Reliable Leak Detector

Citation: Chatzigeorgiou, Dimitris, Kamal Youcef-Toumi, and Rached Ben-Mansour. "Design of a Novel In-Pipe Reliable Leak Detector." IEEE/ASME Transactions on Mechatronics, 2015, volume: 20, Issue: 2, pp.824-833.

As Published: http://dx.doi.org/10.1109/TMECH.2014.2308145

Publisher: Institute of Electrical and Electronics Engineers (IEEE)

Persistent URL: http://hdl.handle.net/1721.1/88034

Version: Author's final manuscript: final author's manuscript post peer review, without publisher's formatting or copy editing

Design of a Novel In-Pipe Reliable Leak Detector

Dimitris Chatzigeorgiou, Kamal Youcef-Toumi and Rached Ben-Mansour

***Abstract*— Leakage is the major factor for unaccounted losses in every pipe network around the world (oil, gas or water). In most cases the deleterious effects associated with the occurrence of leaks may present serious economical and health problems. Therefore, leaks must be quickly detected, located and repaired. Unfortunately, most state of the art leak detection systems have limited applicability, are neither reliable nor robust, while others depend on user experience.**

In this work we present a new in-pipe leak detection system. It performs autonomous leak detection in pipes and, thus, eliminates the need for user experience. This paper focuses on the detection module and its main characteristics. Detection in based on the presence of a pressure gradient in the neighborhood of the leak. Moreover, the proposed detector can sense leaks at any angle around the circumference of the pipe with only two sensors. We validate the concepts by building a prototype and evaluate the system's performance under real conditions in an experimental laboratory setup.

I. Introduction

Potable water obtained through access of limited water reserves followed by treatment and purification is a critical resource to human society. Failure and inefficiencies in transporting drinking water to its final destination wastes resources and energy. In addition to that, there are thousands of miles of natural gas and oil pipelines around the globe that are poorly maintained. Therefore, a significant portion of the total oil and natural gas production is lost through leakage [1]. This causes, among others, threats for humans and damage to the environment.

Pipeline leak may result from bad workmanship or from any destructive cause, due to sudden changes in pressure, corrosion, cracks, defects in pipes or even lack of maintenance [2]. Thus, water utilities as well as gas and oil authorities have been paying serious attention in preventing the loss of their product due to leakages in the pipe network. Over the last 20 years significant amount of research has been conducted towards the development of reliable leak detection techniques.

A. Out-of-Pipe Methods

There are various techniques reported in the literature for leak detection [3], [4]. First, leak losses can be estimated from audits. For instance in the water industry, the difference between the amounts of water supplied to the network by the water company and the total amount of water recorded by water usage meters indicates the amount of unaccounted water. While this quantity gives a good indication of the rate of water leakage in a distribution network, metering gives no information about the locations of the leaks.

Acoustic leak detection is normally used not only to identify but also locate leaks. Acoustic methods consist of listening rods or aquaphones. These devices make contact with valves and/or hydrants. Acoustic techniques may also include geophones in order to listen for leaks on the ground directly above the pipes [4]. Drawbacks of those methods include the necessary experience needed by the operator. The method is not scalable to the network range, since the procedure is very slow.

More sophisticated techniques use acoustic correlation methods, where two sensors are placed on either side of the leak along a pipeline. The sensors bracket the leak and the time lag between the acoustic signals detected by the two sensors is used to identify and locate the leak [5]. This cross-correlation method works well in metal pipes. However, a number of difficulties are encountered in plastic pipes and the effectiveness of the method is doubtful [6], [7].

Finally, several non-acoustic methods like infrared thermography, tracer gas technique and ground-penetrating radar have been reported in the literature of leak detection [8], [9]. Those methods have the advantage of being insensitive to pipe material and operating conditions. Nevertheless, a map of the network is needed, user experience is necessary and the methods are in general slow.

B. In-Pipe Methods

Past experience has shown that in-pipe inspection is more accurate, less sensitive to external noise and also more robust. The latter holds because the detection system comes usually closer to the location of the leaks/defects. In this section various in-pipe leak detection approaches are reported.

The *Smartball* is a mobile device that can identify and locate small leaks in liquid pipelines larger than 6" in diameter constructed of any pipe material [10]. The free-swimming device consists of a porous foam ball that envelops a watertight, aluminum sphere containing the sensitive acoustic instrumentation.

Sahara is able to pinpoint the location and estimate the magnitude of the leak in large diameter water transmission mains of different construction types [11]. Carried by the flow of water, the *Sahara* leak detection system can travel through the pipe. In case of a leak, the exact position is marked on the surface by an operator who is following the device at all times. Both *Smartball* and *Sahara* are passive (not actuated) and cannot actively maneuver inside complicated pipeline configurations. In both cases, operator

D. Chatzigeorgiou is with the Mechatronics Research Lab, Mechanical Engineering Dept., MIT., K. Youcef-Toumi is with Faculty of Mechanical Engineering Dept. and also the director of the Mechatronics Research Lab, MIT {dchatzis, youcef}@mit.edu

R. Ben-Mansour is with Faculty of Mechanical Engineering Dept., KFUPM rmansour@kfupm.edu.sa

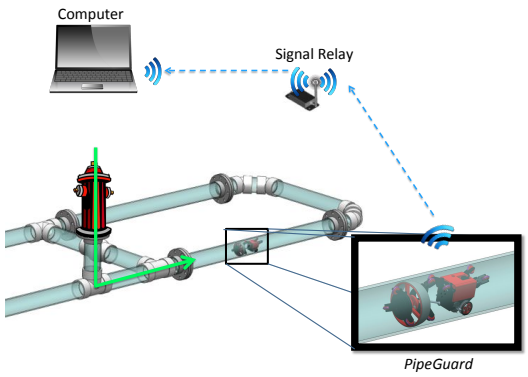

Fig. 1. Pipe health monitoring using *PipeGuard*. *PipeGuard* travels in the network, searches for leaks and transmits signals wirelessly via relay stations to a computer.

experience is needed for signal interpretation and leakage localization.

Our group developed a passive in-pipe inspection system for water distribution networks using acoustic methods [12]. It is designed to operate in small pipes. The merits of the in-pipe acoustic leak detection under different boundary conditions are reported in [13], [14]. Although, there seems to be some promise in such an approach, the method can fail when pipes are made out of plastic material [15], [16].

Under some circumstances it is easier to use remote visual inspection equipment to assess the pipe condition. Different types of robotic crawlers have been developed to navigate inside pipes. Most of these systems utilize four-wheeled platforms, cameras and an umbilical cord for power, communication and control, e.g. the *MRINSPECT* [17]. Schemph et al. report on a long-range, leak-inspection robot that operates in gas-pipelines (*Explorer*) [18]. A human operator controls the robot via wireless RF signals and constantly looks into a camera to search for leaks. Those systems are suitable for gas or empty pipelines (off-line inspection).

In the oil industry several nondestructive testing methods are used to perform pipe inspections. Most systems use magnetic flux leakage based detectors and others use ultrasound to search for pipe defects [19]. These methods' performance depends on the pipe material. They are also power demanding, most of the times not suitable for long-range missions and have limited maneuvering capabilities because of their large size.

In this paper we introduce *PipeGuard*, a new system able to detect leaks in pipes in a reliable and autonomous fashion (Fig. 1). The idea is that *PipeGuard* is inserted into the network via special insertion points. The system inspects the network and sends signals wirelessly via relay stations to a computer [20]. Leak signals stand out clearly on occurrence of leaks, eliminating the need for user experience. The latter is achieved via a detector that is based on identifying a clear pressure gradient in the vicinity of leaks [21], [22]. The system that we describe in this work is optimized to operate in gas/air pipes.

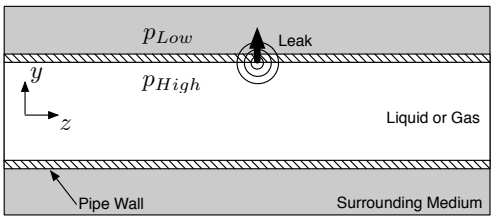

Fig. 2. A simple sketch of a leaking pipe. A leak occurs in on the pipe wall and, thus, fluid is escaping through the opening. Note the notation p_{High} and p_{Low}. Note also that the longitudinal axis of the pipe is z, while the transverse is y.

II. Detection Based on Pressure Gradient

In this section the proposed detection concept and the detector design are discussed. Detection is based on identifying the existence of a localized pressure gradient $({}^{\partial p}/_{\partial r}$, where r stands for the radial coordinate of the pipe). This pressure gradient appears always in pressurized pipes in the vicinity of leaks and is independent of pipe size and/or pipe material. Moreover, the pressure gradient exists in different media inside pipes, which makes the detection method widely applicable (gas, oil, water pipes, etc).

A. Radial Pressure Gradient

For our analysis we consider the case of a straight pipe for simplicity. All results can be extended to bent sections, Y- and T-junctions and other complicated pipe configurations without major changes. Let's consider the case of a straight pressurized pipe section as the one shown in Fig. 2. Lets also assume a leak exists in the middle of the pipe. As one would expect due to the (positive) difference in pressures ($\Delta p = p_{High} - p_{low}$) fluid is escaping from the pipeline through the opening.

In our work we focus on small leaks. This enables us to assume that the line pressure is almost constant across a leakage (in the longitudinal dimension), which is a reasonable assumption for small openings. Not to mention that large leaks can easily be detected by other means. For instance installed pressure sensors around the network can easily sense a large drop in line pressure, that arises in case of a large leak.

The proposed detection concept is based on the fact that any leakage in a pipeline changes the pressure and flow field of the working medium. Our group studied, characterized and quantified the phenomenon in detail [23]. The main conclusion is that the region near the leak that is affected is small. However, this region is characterized by a rapid change in static pressure, dropping from p_{High}, inside the pipeline, to p_{Low} at the surrounding medium resting outside (Fig. 3). The latter phenomenon is essentially a radial pressure gradient.

The local drop in pressure is the key feature in the proposed leak detection scheme. The radial pressure gradient on occurrence of leaks essentially represents a suction region. Numerical studies showed that the radial pressure gradient close to the leak is large in magnitude and drops quickly as distance increases. Fig. 4 shows simulation results for the

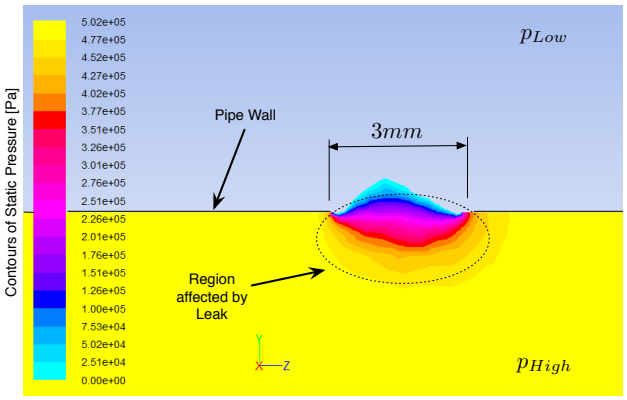

Fig. 3. Numerical study of the static pressure distribution in the vicinity of a $3mm$ leak in a pipe filled with compressed air. In this study $\Delta p = 5bar$.

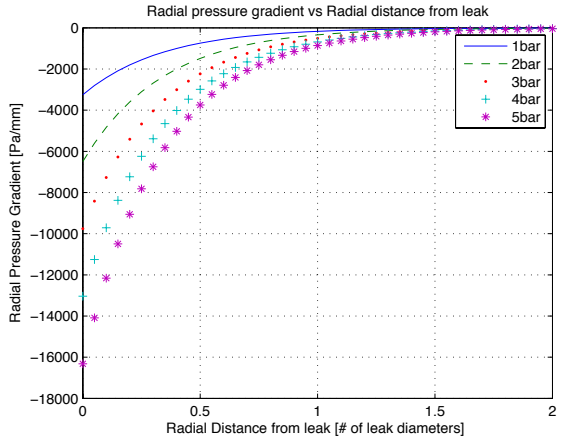

Fig. 4. Numerical studies of the radial pressure gradient in the vicinity of a $3mm$ leak. A compressed air pipe of $100mm$ ID is simulated in this case. Different cases for Δp are shown. The magnitude of the radial pressure gradient drops quickly with distance.

radial pressure gradient as a function of radial distance from a $3mm$ circular leak.

Identifying leaks based on this radial pressure gradient proves to be reliable and effective as shown in this paper. Directly measuring the pressure at each point in order to calculate the gradient is not efficient and should be avoided. However, as a leak can happen at any angle ϕ around the circumference, full observability would require a series of pressure sensors installed around the perimeter of the pipe. To avoid the complexity of such an attempt, we introduce a more efficient mechanism in the next section.

B. Detector Concept

In this section we present our detection concept for the identification of the radial pressure gradient in case of leaks. The main requirement is that the system should be able to detect leaks at any angle ϕ around the circumference of the pipe.

A schematic of the proposed detection concept is shown in Fig. 5. To achieve full observability around the circumference a circular membrane is utilized. The membrane is moving

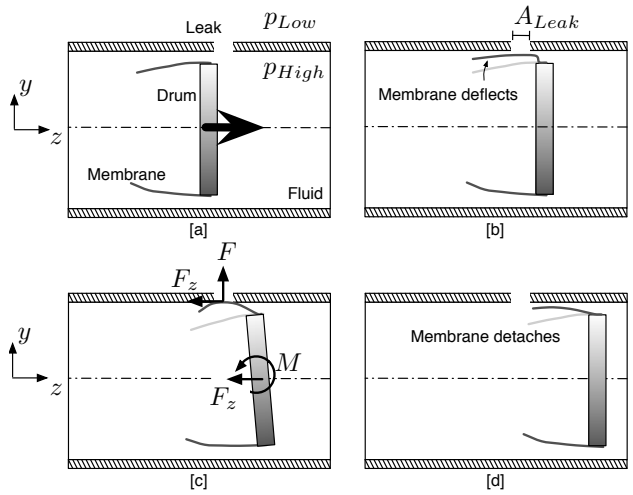

Fig. 5. The detection concept: [a] "Approach Phase": The detector is moving from left to right with the help of the carrier. Only the drum and the membrane are depicted for simplicity. [b] "Detection Phase A": The membrane is pulled towards the leak due to the suction caused by the drop in pressure. [c] "Detection Phase B": The membrane touches the walls and covers the leak. As *PipeGuard* moves along the pipe a new force, F_z is generated. [d] "Detaching Phase": The membrane detaches from the leak and the drum returns to the initial position.

close to the pipe walls at all times complying to diameter changes and other defects on the walls, e.g. accumulated scale. The membrane is suspended by a rigid body, called drum (Fig. 5 [a]). The drum is allowed to rotate about its center point G (about any axis) by design. The latter is allowed by a gimbal mechanism.

In case of a leak, the membrane is pulled towards it (because of the presence of a suction force caused by the pressure gradient $[\partial p/\partial r]$ as described earlier) (Fig. 5 [b]). Upon touching the walls, a pressure difference Δp is creating the normal force F on the membrane. We can write that:

$$F = \Delta p A_{Leak} \tag{1}$$

where A_{Leak} stands for the cross-sectional area of the leak, which can be of any shape.

As *PipeGuard* continues traveling along the pipe, a new force is generated (F_z). This force is a result of friction between the membrane and the pipe walls. F_z is related to the normal force, F, by an appropriate friction model, say $F_z = g(F)$. The analytic form of function g is not discussed in this paper. By using Eq. (1) we can see that F_z depends on the pressure difference, since $F_z = g(\Delta p A_{Leak})$.

Furthermore, F_z generates an equivalent force and torque on the drum, M, a key fact that is discussed further in the coming sections. As a result, M forces the drum to rotate about some axis passing through its center, while orientation of the axis depends on the angle ϕ of the leak around the circumference (Fig. 5 [c]). The effects of M can be sensed by force and/or displacement sensors mounted on the detector. F_z only vanishes when the membrane detaches from the leak and the drum bounces back to the neutral position (Fig. 5 [d]).

In the next section we describe the detailed design of

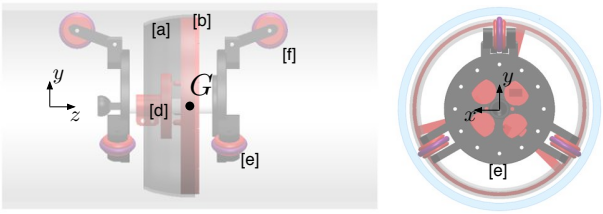

Fig. 6. 3D solid model of the proposed detector. Side and front view in a pipe. Details: [a] Membrane, [b] Drum, [d] Sensor Chassis and [e] Carrier, [f] Suspension Legs

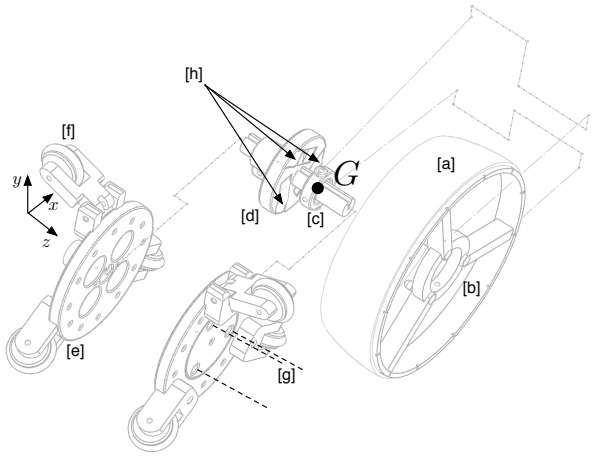

Fig. 7. The exploded view of the proposed design. All key components are laid out. Details: [a] Membrane, [b] Drum, [c] Gimbal, [d] Sensor Chassis, [e] Carrier, [f] Suspension Legs, [g] Axes of Linear Springs, [h] Supporting Points for Drum

a mechanism that utilizes the concept presented here to effectively identify leaks in pipes. The proposed system can identify a leak by measuring forces on the drum. Essentially, the problem has switched from identifying a radial pressure gradient (at any angle ϕ), to measuring forces on a mechanism.

III. Detector Design

This section discusses the design and the analysis of the system proposed in this paper.

A. Design Overview

A 3D solid model of the proposed detector is shown in Fig. 6. The exploded view of the design is presented in Fig. 7. The drum is depicted in red (solid color) and the membrane in dark grey (transparent color). The drum is suspended by a wheeled system and remains always in the middle of the pipe. A key factor in this proposed design is the gimbal mechanism consisting of two different parts (parts [b] and [c] in Fig. 7). This mechanism allows the drum to pivot about two axes and thus respond to any torque, M, about any axis passing through its center point G. Moreover, the system dimensions are such that the membrane leaves a small clearance ($< 2mm$) from the walls of the pipe.

Whenever a leak exists, a torque M is generated about some axis on the drum depending on the leak angle, ϕ,

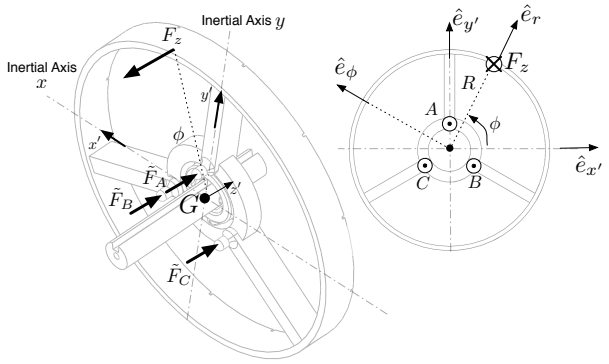

Fig. 8. Forces acting on the drum in case of a leak and a corresponding force F_z. A 3D view as well as a front view (side) is shown

as described earlier. M is sensed by appropriate sensors on the back plate on the carrier. Very small motions on the drum are allowed in this specific embodiment. Springs are used in order to push the drum back to the neutral position after detection is completed (Fig. 5 [d]). In this proposed embodiment three linear springs are used and they are omitted in all figures for simplicity. However, the axes of the springs are shown in Fig. 7.

B. Detector Analysis

In this section we present the analysis of the forces acting on the detector and justify the placement of sensors on the final design. In addition we propose a detection algorithm/metric for effective leak detection.

1) Force Analysis: In this work we perform a first order statics discussion on the detector. We assume that the drum is only allowed to perform small rotations and, thus, the analysis is accurate when the motion of the drum is small and its dynamics are considered insignificant.

We discussed earlier that a force $\mathbf{F_z} = -F_z\hat{\mathbf{e}}_\mathbf{z}$ is generated at leak positions[1]. This force is then generating a torque about point G, the center of the gimbal mechanism, which is equal to (see Fig. 8):

$$\begin{aligned}\mathbf{M} &= F_z R\hat{\mathbf{e}}_\phi \\ &= F_z R(cos\phi\hat{\mathbf{e}}_\mathbf{y} - sin\phi\hat{\mathbf{e}}_\mathbf{x})\end{aligned} \tag{2}$$

On the other hand, the drum is supported at three points, namely points A, B and C (Fig. 8). The distance between each of these points and the center of the gimbal G is the same and equal to r. In addition, those points are $2\pi/3$ away from each other. Moreover, points A, B and C are the points where the springs are mounted (on the other side of the drum). By adjusting the pre-loading on the springs, we can independently adjust the corresponding mean forces on the supports ($\bar{F}_A, \bar{F}_B, \bar{F}_C$) at the neutral position (no leak).

However when a leak incidence occurs, a disturbance torque M stemming from F_z arises. This torque changes

[1]Here we use $\hat{\mathbf{e}}_\mathbf{z}$ to represent the unit vector along axis z and similar notation will be followed in rest of the work.

the support forces at points A, B and C, by $\tilde{F}_A, \tilde{F}_B$ and $\tilde{F}_C$ correspondingly. We can write:

$$\tilde{\mathbf{M}}_{\mathbf{x}} = [\tilde{F}_A r - (\tilde{F}_B + \tilde{F}_C) r sin(\pi/6)]\hat{\mathbf{e}}_{\mathbf{x}} \quad (3)$$

$$\tilde{\mathbf{M}}_{\mathbf{y}} = [\tilde{F}_C - \tilde{F}_B] r cos(\pi/6)]\hat{\mathbf{e}}_{\mathbf{y}} \quad (4)$$

And the total change in the support torque due to the leak incidence is equal to:

$$\tilde{\mathbf{M}}_{\mathbf{support}} = \tilde{\mathbf{M}}_{\mathbf{x}} + \tilde{\mathbf{M}}_{\mathbf{y}} \quad (5)$$

In the previous notation we implied that for the total support force at point A we can write:

$$F_A = \bar{F}_A + \tilde{F}_A$$

where the first component stands for the mean value ($\bar{F}_A$), that is apparent at all times due to pre-loading of the spring mounted at point A. The latter component ($\tilde{F}_A$) arises only at leak incidents and represents the change in the force due to the disturbance from the leak. Similar notation can be written for the support forces at points B and C as well.

We assume for this analysis that the drum is only allowed to perform small movements and, thus, static analysis is accurate to first order. To complete the analysis we need to equilibrate the torques and forces acting on the system in case of a leak incidence. To do this we need to set $\tilde{\mathbf{M}}_{\mathbf{support}} = \mathbf{M}$, using Eq. (2-5).

In addition, we assume that F_z is balanced by the support provided by the axes of the gimbal at point G. So we can write for the sum of the three changes in the support forces at points A, B and C:

$$\tilde{F}_A + \tilde{F}_B + \tilde{F}_C \approx 0 \quad (6)$$

We can now solve the system of equations for the three unknown support forces:

$$\tilde{\mathbf{F}}_{\mathbf{A}} = \frac{-2Rsin\phi}{3r} F_z \hat{\mathbf{e}}_{\mathbf{z}} \quad (7)$$

$$\tilde{\mathbf{F}}_{\mathbf{B}} = R\frac{sin\phi - \sqrt{3}cos\phi}{3r} F_z \hat{\mathbf{e}}_{\mathbf{z}} \quad (8)$$

$$\tilde{\mathbf{F}}_{\mathbf{C}} = R\frac{sin\phi + \sqrt{3}cos\phi}{3r} F_z \hat{\mathbf{e}}_{\mathbf{z}} \quad (9)$$

By looking at Eq. (7-9) one can conclude that depending on the value of the incidence angle ϕ, the signals captured by appropriate force sensors mounted at points A, B and/or C are different in amplitude and phase. For completeness, we need to mention that the forces that are sensed by force sensors installed on the detector's sensor chassis (see Fig. 7/Part [d]) are always opposite in sign from the support forces calculated in Eq. (7-9). We can write:

$$\tilde{\mathbf{F}}_{\mathbf{A}}^{\mathbf{Sensor}} = -\tilde{\mathbf{F}}_{\mathbf{A}} = \frac{2Rsin\phi}{3r} F_z \hat{\mathbf{e}}_{\mathbf{z}} \quad (10)$$

$$\tilde{\mathbf{F}}_{\mathbf{B}}^{\mathbf{Sensor}} = -\tilde{\mathbf{F}}_{\mathbf{B}} = R\frac{\sqrt{3}cos\phi - sin\phi}{3r} F_z \hat{\mathbf{e}}_{\mathbf{z}} \quad (11)$$

$$\tilde{\mathbf{F}}_{\mathbf{C}}^{\mathbf{Sensor}} = -\tilde{\mathbf{F}}_{\mathbf{C}} = -R\frac{sin\phi + \sqrt{3}cos\phi}{3r} F_z \hat{\mathbf{e}}_{\mathbf{z}} \quad (12)$$

For the demonstration part at the end of this paper we built a prototype that is designed to operate in $100mm$ ID gas pipes and has the following dimensions:

$$R = 47mm$$
$$r = 12.5mm$$

2) Sensor Placement & Algorithm: By installing two force sensors on the supports we are able to measure the corresponding forces directly. The idea is to measure the support forces as a result of the leak force F_z, instead of measuring the leak pressure gradient directly.

To avoid "blind spots" and to be able to detect leaks at any angle around the circumference the system needs to perform at least two force measurements. The latter statement needs to be proven via observability analysis, which is outside the scope of this paper. However, one can think of the simple case of a single leak at $\phi = 0^o$. In such case a force sensor installed on point A would not give any change in the measurement ($\tilde{F}_A^{Sensor} = 0$ for $\phi = 0^o$). However, another sensor placed on either point B or C will be able to measure change in the signals due to the leak and, thus, the detector will be able to eventually identify the leak/defect in the pipe.

In this embodiment we install force sensors on points B and C without loss of generality (we could have picked any 2 points between A, B and C). In addition we propose the use of the following metric in order to effectively trigger alarms in case of leaks:

$$J(t,T) = \int_{t-T}^{t} \sqrt{\tilde{F}_B^{Sensor}(\tau)^2 + \tilde{F}_C^{Sensor}(\tau)^2} d\tau \quad (13)$$

where T is the integration period. Whenever $J(t,T) > c$, where c is a predefined constant, a leak is identified. c represents a threshold, above which an alarm is triggered and the existence of a leak is assumed. This quantity needs to be selected in such a way, in order to neglect noise and at the same time avoid false positives. However, large values of c will lower the sensitivity of the detection. This metric (Eq. 13) essentially represents a moving window of integration of the changes in signals of the two installed force sensors.

IV. Prototype & Instrumentation

For this work *PipeGuard* is designed to operate in $100mm$ ID gas pipes. However, all concepts discussed in this paper can be scaled and slightly altered accordingly to accommodate pipes of different sizes and perform leak inspection in other fluid media, e.g. water. In the following paragraphs the complete autonomous system, namely PipeGuard, is described in detail.

A. PipeGuard's Carrier

PipeGuard consists of two modules, i.e. the carrier and the detector (Fig. 9). The detector design and concepts were discussed in detail in previous sections. The carrier assures the locomotion of the system inside the pipe. The module is carrying actuators, sensors, power and also electronics for

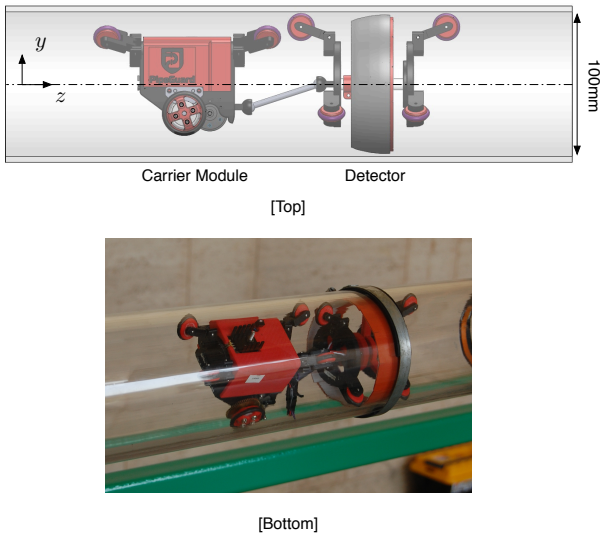

Fig. 9. Side view of *PipeGuard*. [Top]: Solid Model. A pipe section is drawn for reference. [Bottom]: The actual developed prototype inside a $100mm$ ID pipe.

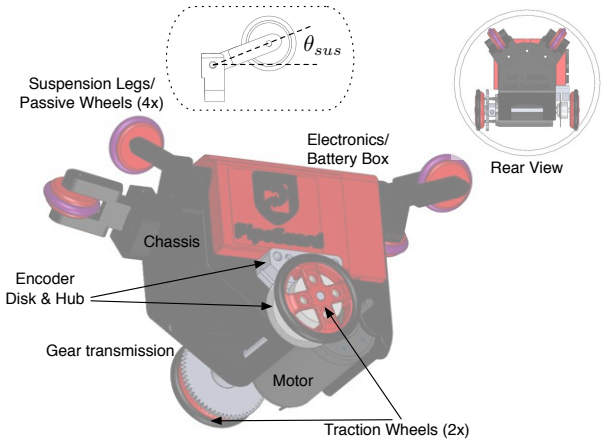

Fig. 10. A 3D solid model of the carrier module. A sketch of the carrier's rear view inside a $100mm$ ID pipe is shown in the top right.

signal processing and communications. A 3D solid model of the carrier along with explanations of its main subsystems is presented in Fig. 10.

The module's locomotion is materialized via a pair of traction wheels ($OD = 1\ 3/16'' \approx 30.1mm$) (Fig. 10). Those two wheels are touching the lower end of the wall. In addition, the system is suspended by four legs with passive rollers from the upper walls as shown in the same figure.

Each suspension wheel has a spring loaded pivot. The angle θ_{sus} of each pivot point on each suspension wheel is regulated in a passive way and is providing the required compliance to the carrier. That compliance is very important, since it enables the module to align itself properly inside the pipe, overcome misalignments or defects on the pipe walls or even comply with small changes in the pipe diameter.

The main actuator of the module is a $20W$ brushed DC Motor from "Maxon" (339150). The motor is connected to the traction wheels via a set of gears with ratio 5:1. In order to regulate speed, an incremental rotary encoder (50 counts) from "US Digital" is used and the speed loop is closed. Both disk and hub are shown in Fig. 10. Finally, all electronics, communication modules and batteries are housed inside the carrier module.

B. Electronics Architecture

Derived from our design requirements, the robot should be able to perform the following tasks:

- Move and regulate the speed inside pipes
- Identify leaks by measuring signals from two force sensors at relatively high sampling rates.
- Communicate with the "Command Center" (computer) wirelessly

PipeGuard's architecture is developed to meet these requirements and is shown in Fig. 11. To perform the aforementioned tasks two micro-controllers are used. Micro-controller #2 is dedicated to speed regulation and micro-controller #1 is performing real-time leak sensing.

The workflow is the following: The user specifies a motion command on the computer. The computer sends out the motion command including desired speed and desired position to *PipeGuard*. After the WiFi transceiver on the robot receives the command, it delivers the command to micro-controller #2. Micro-controller #2 performs closed loop speed control in order to regulate speed of the carrier. At the same time it calculates speed (by measuring the signal from the encoder) and commands the system to stop if it reaches the end of the pipe section (or any other point along the pipe as specified by the operator).

Parallel to micro-controller #2, micro-controller #1 is responsible for leak detection and for sending out sensor data to the WiFi transceiver. This micro-controller receives signals from the two force sensors installed on the detector. At the same time it receives the measured position from the encoder mounted on the carrier. It compiles the correlated force sensor data with position data and sends them out through the WiFi transceiver. The WiFi receiver on the command center then receives the data, decomposes them and supplies them to the user via the graphical user interface on the computer.

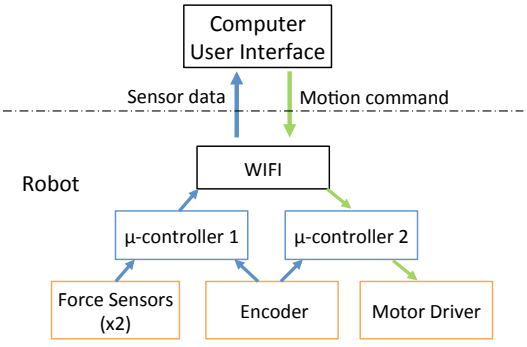

Fig. 11. High level system architecture of *PipeGuard*. Two micro-controllers are installed on the system for simultaneous speed regulation and leak detection.

The WiFi transceiver that we selected is an Xbee Pro 900MHz RF module. We use two Arduino Pro Mini 328 5V/16MHz and the motor driver under codename VNH5019 from Polulu. The whole system is powered by a 11.1V 350 mAh 65C Li-polymer battery. Finally, we use two FSR (Force Resistive Sensors) 400 force sensors for leak detection from "Interlink Electronics". The latter ones are powered at 5V and a resistor of $8k\Omega$ is used for the necessary voltage division. The calibration curve for those sensors is shown in Fig. 12. The whole system (Carrier and Detector) can run for 30mins with this configuration, performing leak inspection and locomotion inside pipelines.

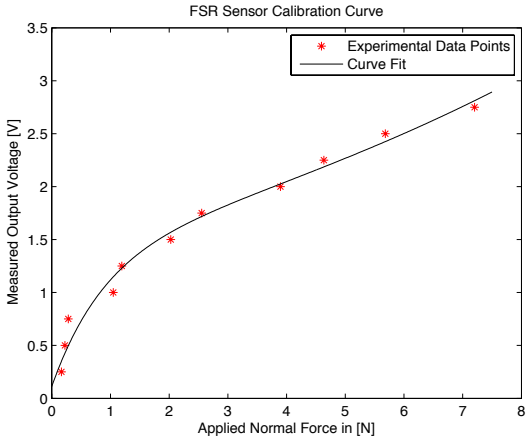

Fig. 12. Calibration curve and experimental data points for FSR 400 sensor from "Interlink Electronics". The latter one is powered at 5V and a resistor of $8k\Omega$ is used for voltage division.

V. Experimental Validation

In this section we evaluate *PipeGuard* in an experimental setup. The setup consists of a straight $100mm$ ID and $1.40m$ long PVC pipe. The system is deployed in the pipe and performs leak detection in a pressurized air environment. Artificial leaks have been created on the pipe walls in the shape of circular $2mm$ and $3mm$ openings. Those openings can be considered small for the general case and usually such leaks fail to be detected by most state-of-the-art systems.

A picture of *PipeGuard* inside the experimental setup is shown in Fig. 13. *PipeGuard* moves along the pipe from [Start] to [End] and its job is to identify the leaks. In Fig. 13 leak #1 is covered/sealed and leak #2 is opened/active.

A. Understanding Leak Signals

Initially we demonstrate detection results with the system moving at very slow speeds in the pipe. In this case the detector passes by consecutive openings/leaks of $2-3mm$ in diameter. The line pressure during the experiments was always constant and equal to 1.4bar.

During experimentation we observe that the detector is able to capture signals that clearly indicate the existence of leaks. The initial results are indeed promising. Signals are presented in Fig. 14 for two different cases. In every case the leak signals ($\tilde{F}_B^{Sensor}$ and $\tilde{F}_C^{Sensor}$) stands out of the

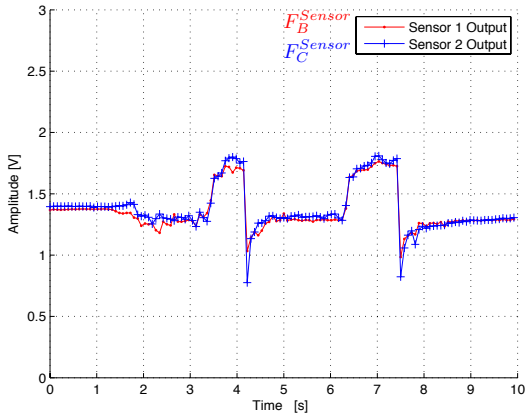

(a)

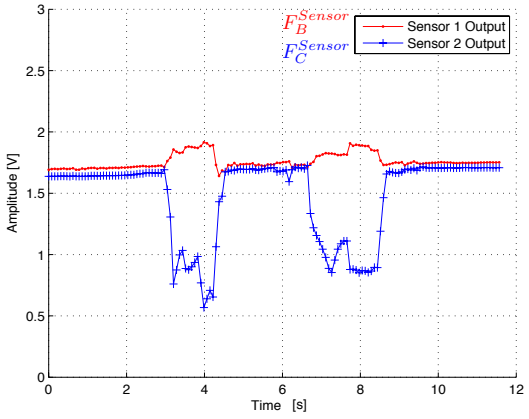

(b)

Fig. 14. Signals captured by the 2 FSR sensors during initial experiments. (a) Sensor runs across two leaks at an angle of $\phi \approx 270^o$. Thus, the leak signals are in phase. (b) Sensor runs across two leaks at an angle of $\phi \approx 45^o$ and signals are out of phase.

mean values ($\bar{F}_B^{Sensor}$ and $\bar{F}_C^{Sensor}$) and clear peaks can be observed for the raw, unfiltered data. By preloading the springs on the detector we adjusted the mean values to be around $1.5V$ for each one of the two experiments.

More specifically, in Fig. 14(a) we present the signals captured by the two sensors when the system came across two similar leaks at an angle $\phi \approx 270^o$. Whenever the system encounters a leak the response of the sensing elements and the forces captured look similar (from Eq. (11, 12) we get that $\tilde{F}_B = \tilde{F}_C$ for $\phi = 270^o$). We can see that in this case the initial response of the signal to a leak is increasing in magnitude and when the flexible material detaches comes back to the mean/preloaded value ($\bar{F}_B^{Sensor}$ and $\bar{F}_C^{Sensor}$). This indicates that forces on both sensors are of pushing nature.

In Fig. 14(b) we plot the signals captured by the two sensors when the system comes across two similar leaks at an angle $\phi \approx 45^o$ around the circumference. Again the signals have the same trends between leak instances. In this case the signals captured by the two sensors seem to be behaving

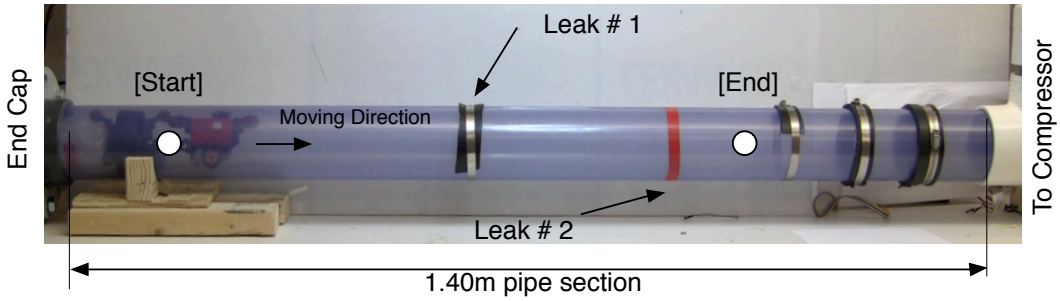

Fig. 13. The experimental setup we used for the evaluation of *PipeGuard*. The system moves along the pipe from [Start] to [End] and performs leak detection. Along this path there are two potential leaks to be detected. In this specific picture leak #1 is covered and closed, while leak #2 is open and active.

in an opposite manner, namely as the one drops the other rises in magnitude at each leak (signals out of phase). This indicates that force on sensor 1 is of pushing, while the force on sensor 2 is of pulling nature.

The differences between the two experiments exist due to the fact that each leak is at a different angle and this results in a different pair of F_z and M about G as discussed in previous sections. Since the sensors are placed at different positions on the carrier's back plate one can design and develop estimation algorithms for estimating the position (incidence angle ϕ) and the magnitude of the leaks. Nevertheless, it is now clear that whenever the system passes by a leakage, a clear change in signal(s) will pinpoint the existence of a leakage, as expected. To quantify this phenomenon a metric (Eq. 13) is used in the coming sections.

B. Low Speed Detection

The next step is to let the system (carrier + detector) run in the pipe at relatively higher, but still low speeds. We command *PipeGuard* to move at $\omega_d = 2Hz$, which is equivalent to a desired linear speed $v_d = 0.19m/s$. At this speed the system is able to traverse the distance from [Start] to [End] in approximately $5s$. The signals captured by the two force sensors are shown in Fig. 15. Note that in this case the mean values are eliminated (filtered out) for simplicity (this will be done in all coming experiments without mentioning). Again, a clear change in the signals reveals the existence of a leak in the pipe. Note here that for this experiment the line pressure was regulated to be equal to $1bar$. In the same figure the evolution of the proposed metric from Eq. (13) is shown. A clear peak above the noise level is indicating the existence of a leak at $t = t^*$, when $J(t^*, T = 0.2s) > 0.025$.

As *PipeGuard* approaches the leak, noise can corrupt the signals, but is much smaller in amplitude than the leak signal (Fig. 15). Detection occurs in four phases. Initially *PipeGuard* approaches the leak. Then the membrane is moving towards the leak because of the effect of the radial pressure gradient. The latter small movement results in a small change in the signals (undershoot in this case). When the membrane touches the wall at the leak position, a force F_z is generated, resulting in the torque M on the drum. The latter torque pushes the drum to move and, thus, the

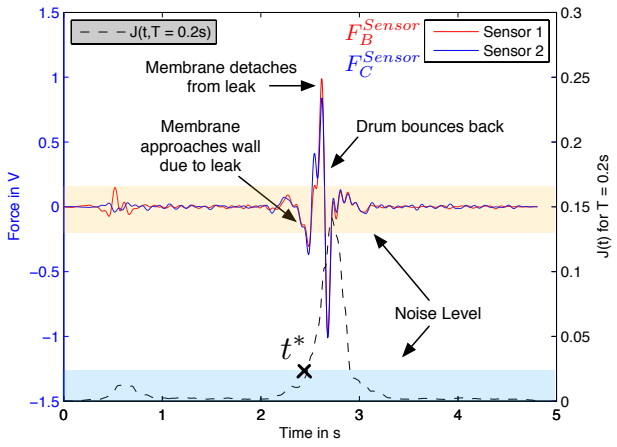

Fig. 15. Sensor signals as *PipeGuard* moves along the pipe. Signals presented here are collected at 160Hz for each sensor. Line pressure is equal to $1bar$. In addition the metric $J(t, T = 0.2s)$ is plotted here. Leak is successfully identified.

signals of the two force sensors change significantly. Signals continue to increase up to a certain point when the membrane detaches from the leak. At this point the drum bounces back to the neutral position and signals return to their nominal (mean) values.

Another experiment showed that successful detection is performed too, when both leaks along the pipe are opened. Again *PipeGuard* is commanded to move at $v_d = 0.19m/s$. The detector passes by the two consecutive leaks and the signals captured are presented in Fig. 16. Signal magnitude for leak #1 is smaller than the magnitude for leak #2. This is expected, as line pressure at the position of leak #1 is reduced, because of the existence of leak #2. By carefully selecting corresponding thresholds c, one can trigger alarms at times t_i^* when $J(t_i^*, T) > c$. In this case, again, $c = 0.025$ is selected in order to avoid false positives (neglect noise) and effectively trigger alarms at leak locations.

By carefully observing Fig. 16 we can see that signals captured as *PipeGuard* is passing by the first leak are in phase, while the signals at the second leak are out of phase. This occurs because the two leaks are at a different angle on

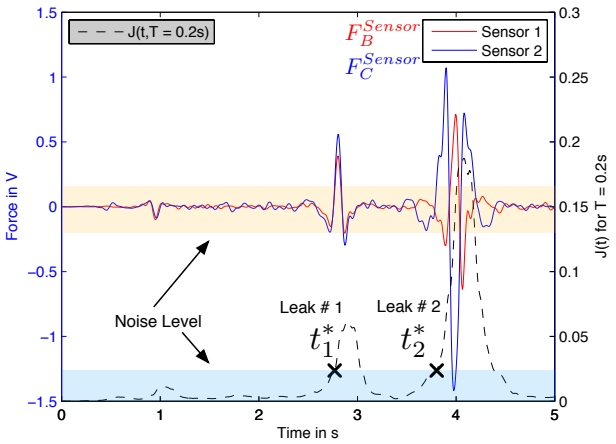

Fig. 16. Sensor signals as *PipeGuard* moves along the pipe. Signals presented here are collected at 160Hz for each sensor. Line pressure (at the compressor) is equal to $1.4bar$. Sensor signals are in phase for leak #1 and out of phase for leak #2. In addition the metric $J(t, T = 0.2s)$ is plotted here. Two leaks are successfully identified.

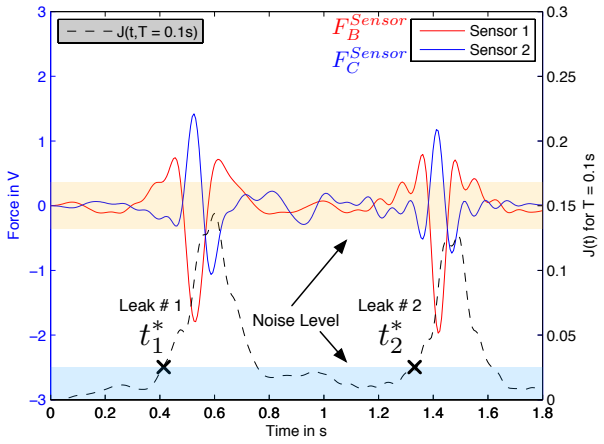

Fig. 17. Sensor signals as *PipeGuard* moves along the pipe. Signals presented here are collected at 160Hz for each sensor. Line pressure (at the compressor) is equal to $1.4bar$. *PipeGuard* is moving at approximately $0.875m/s$ inside the pipe. In addition the metric $J(t, T = 0.1s)$ is plotted here. Two leaks are successfully identified.

the circumference of the pipe ($\phi_1 \neq \phi_2$).

C. High Speed Detection

PipeGuard is able to move inside the pipes at relatively high speeds. Experimentation showed that *PipeGuard's* motor is saturated at approximately $\omega_d = 9.23Hz$, which is equivalent to $v_d = 0.875m/s$. At this speed *PipeGuard* is able to inspect pipes at a rate of more than $3km$ per hour.

Even at these high speeds *PipeGuard* is still able to inspect pipelines and detect leaks in a reliable fashion. By carefully selecting the triggering thresholds one is able to trigger alarms only when leaks are present and avoid false positives. Example leak signals captured at those high speeds are shown in Fig. 17. In this cases the level of the noise is higher, but still leak signals stand out significantly. In this case $c = 0.025$, but one would probably try to increase threshold in order to avoid any potential false positives. The latter would enable the sensor to neglect higher noise levels, always at the cost of reducing the sensitivity of detection.

VI. Conclusions and Future Work

In this paper a leak detection concept and design are proposed and discussed. It is claimed in the beginning that the system is able to detect leaks in a reliable and robust fashion, because of the fundamental principle behind detection. More specifically, the detection principle is based on identifying the existence of a localized pressure gradient, which is apparent in pressurized pipes in the neighborhood of leaks. In the proposed system the detection is independent of pipe size and pipe material, unlike many of the current methods.

Directly measuring the pressure at each point in order to calculate the gradient is not efficient. In addition, as a leak can happen at any angle around the circumference, full observability would require a series of pressure sensors installed around the circumference of the pipe. To overcome such complexity we propose and design a smart mechanism that "shifts" the problem from directly measuring the pressure at each point around the circumference, to measuring the forces on a mechanism.

We built and tested a prototype in a laboratory setup. The system can successfully identify leaks based on the radial pressure gradient. Small consecutive leaks were detected accurately even at relatively low pressures and high speeds. At higher pressures the signal to noise ratio is higher and the detection becomes more reliable and robust. Finally, a metric to quantify leak signals and trigger alarms at leak locations is proposed and proved to be effective.

Our future work includes the refinement and optimization of the design of the detector in order to increase its sensitivity to lower pressures. In addition to that, we are in the process of designing a "compliant drum". The latter one is going to be able to adjust its size to the actual diameter of the pipe and comply with any sharp changes in the nominal ID, extrusions, obstacles or even accumulated scale in the pipe. Moreover, we plan to continue working on this technology for both gas and water applications and possibly other types of media. Since experimentation was limited to straight pipelines thus far, we plan to conduct extensive tests in different environments and pipe configurations.

Acknowledgments

The authors would like to thank You Wu. His help is greatly appreciated in this work. In addition, the authors would like to thank Frederick Moore, an undergraduate student at MIT, for his help and support in this project.

The authors would like to thank the King Fahd University of Petroleum and Minerals in Dhahran, Saudi Arabia, for funding the research reported in this paper through the Center for Clean Water and Clean Energy at MIT and KFUPM under Project Number R7-DMN-08.

Last but not least, the first author would like to thank the Onassis Public Benefit Foundation for the award of a prestigious scholarship throughout this work.

REFERENCES

[1] P.-S. Murvay and I. Silea, "A survey on gas leak detection and localization techniques," *Journal of Loss Prevention in the Process Industries*, vol. 25, no. 6, pp. 966 – 973, 2012. [Online]. Available: http://www.sciencedirect.com/science/article/pii/S0950423012000836

[2] Georgia Environmental Protection Division, Watershed Protection Branch, *Water Leak Detection and Repair Program*. EPD Guidance Document, 2007.

[3] Mays L., *Water Distribution Systems Handbook*. McGraw-Hill, 2000.

[4] Hunaidi O., Chu W., Wang A. and Guan W., "Leak detection method for plastic water distribution pipes," *Advancing the Science of Water, Fort Lauderdale Technology Transfer Conference, AWWA Research Foundation*, pp. 249–270, 1999.

[5] Fuchs H. V. and Riehle R., "Ten years of experience with leak detection by acoustic signal analysis," *Applied Acoustics*, vol. 33, pp. 1–19, 1991.

[6] Hunaidi O. and Chu W., "Acoustical characteristics of leak signals in plastic water distribution pipes," *Applied Acoustics*, vol. 58, pp. 235–254, 1999.

[7] Bracken M. and Hunaidi O., "Practical aspects of acoustical leak location on plastic and large diameter pipe," *Leakage 2005 Conference Proceedings*, no. 448-452, 2005.

[8] Hunaidi O., Chu W., Wang A. and Guan W., "Detecting leaks in plastic pipes," *Journal - American Water Works Association*, vol. 92, no. 2, pp. 82–94, 2000.

[9] Hunaidi O. and Giamou P., "Ground-penetrating radar for detection of leaks in buried plastic water distribution pipes," *Seventh International Conference on Ground Penetrating Radar (GPR'98)*, pp. 783–786, 1998.

[10] Kurtz D. W., "Developments in a free-swimming acoustic leak detection system for water transmission pipelines," *ASCE Conf. Proc.*, vol. 25, no. 211, 2006.

[11] Bond A., Mergelas B. and Jones C., "Pinpointing leaks in water transmission mains," *ASCE Conf. Proc.*, vol. 91, no. 146, 2004.

[12] Chatzigeorgiou D., Youcef-Toumi K., Khalifa A. and Ben-Mansour R., "Analysis and design of an in-pipe system for water leak detection," *ASME International Design Engineering Technical Conferences & Design Automation Conference (IDETC/DAC2011)*, 2011.

[13] Khalifa A., Chatzigeorgiou D., Youcef-Toumi K., Khulief Y. and Ben-Mansour R., "Quantifying acoustic and pressure sensing for in-pipe leak detection," *ASME International Mechanical Engineering Congress & Exposition (IMECE2010)*, 2010.

[14] Chatzigeorgiou D., Khalifa A., Youcef-Toumi K. and Ben-Mansour R., "An in-pipe leak detection sensor: Sensing capabilities and evaluation," *ASME/IEEE International Conference on Mechatronic and Embedded Systems and Applications (MESA2011)*, 2011.

[15] J. Muggleton and M. Brennan, "Leak noise propagation and attenuation in submerged plastic water pipes," *Journal of Sound and Vibration*, vol. 278, pp. 527–537, 2004.

[16] R. P. J.M. Muggleton, M.J. Brennan and Y. Gao, "A novel sensor for measuring the acoustic pressure in buried plastic water pipes," *Journal of Sound and Vibration*, vol. 295, pp. 1085–1098, 2006.

[17] Choi H-R. and Roh S-G, "Differential-drive in-pipe robot for moving inside urban gas pipelines," *Transactions on Robotics*, vol. 21, no. 1, 2005.

[18] Schempf H., Mutschler E., Goltsberg V., Skoptsov G., Gavaert A. and Vradis G., "Explorer: Untethered real-time gas main assessment robot system," *Proc. of Int. Workshop on Advances in Service Robotics (ASER)*, 2003.

[19] J. M. Mirats Tur and W. Garthwaite, "Robotic devices for water main in-pipe inspection: A survey," *Journal of Field Robotics*, vol. 27, no. 4, pp. 491–508, 2010. [Online]. Available: http://dx.doi.org/10.1002/rob.20347

[20] Wu D., Youcef-Toumi K., Mekid S. Ben Mansour R., "Relay node placement in wireless sensor networks for pipeline inspection," *IEEE American Control Conference (ACC2013)*, 2013.

[21] Chatzigeorgiou D., Ben-Mansour R., Khalifa A. and Youcef-Toumi K., "Design and evaluation of an in-pipe leak detection sensing technique based on force transduction," *ASME International Mechanical Engineering Congress & Exposition (IMECE2012)*, 2012.

[22] Chatzigeorgiou D., Wu Y., Youcef-Toumi K. and Ben Mansour R., "Reliable sensing of leaks in pipelines," *ASME Dynamic Systems and Controls Conference (DSCC)*, 2013.

[23] Ben-Mansour R, M.A. Habib, A. Khalifa, K. Youcef-Toumi and D. Chatzigeorgiou, "A computational fluid dynamic simulation of small leaks in water pipelines for direct leak pressure transduction," *Computer and Fluids*, p. doi:10.1016/j.compfluid.2011.12.016, 2012.